

**Atomic force microscopy detection of molecular complexes in multiprotein  
P450cam-containing monooxygenase system.**

Vadim Yu. Kuznetsov<sup>1</sup>, Yuri D. Ivanov<sup>1</sup>, Victor A. Bykov<sup>2</sup>, Sergey A. Saunin<sup>2</sup>, Igor  
A. Fedorov<sup>2</sup>, Sergey V. Lemeshko<sup>2</sup>, Hui Bon Hoa<sup>3</sup> and Alexander I. Archakov<sup>1</sup>

<sup>1</sup> – Institute of Biomedical Chemistry, Moscow, Russia

<sup>2</sup> – NT-MDT, Moscow, Russia

<sup>3</sup> – INSERM U 473 84, rue de General Leclerc, Le Kremlin Bicetre, France

Short running title:

Atomic force microscopy detection of complexes in a P450cam system.

**Correspondence:**

Dr. Yu.D. Ivanov

Institute of Biomedical Chemistry RAMS, Pogodinskaya st. 10, Moscow, 119832,  
Russia,

**Fax:** (095) 245-08-57

**E-mail:** [yuiv@ibmh.msk.su](mailto:yuiv@ibmh.msk.su)

**Abbreviations:** **AFM**, atomic force microscopy; **P450cam**, cytochrome  
P450cam; **Pd**, putidaredoxin; **PdR**, putidaredoxin reductase.

**Key words:** cytochrome P450cam / putidaredoxin / putidaredoxin  
reductase / atomic force microscopy / complex formation.

## SUMMARY

The application of atomic force microscopy (AFM) technique in proteomic researches, identification and visualization of individual molecules and molecular complexes within P450cam-containing monooxygenase system was demonstrated. The method makes possible the distinguishing between the binary protein complexes and appropriate monomeric proteins and, also, between the binary and ternary complexes. The AFM images of the components of a cytochrome P450cam-containing monooxygenase system - cytochrome P450cam (P450cam), putidaredoxin (Pd) and putidaredoxin reductase (PdR) - were obtained on a mica support. The molecules of P450cam, Pd and PdR were found to have typical heights of  $2.6 \pm 0.3$  nm,  $2.0 \pm 0.3$  and  $2.8 \pm 0.3$  nm, respectively. The measured heights of the binary Pd/PdR and P450cam/PdR complexes were  $4.9 \pm 0.3$  nm and  $5.1 \pm 0.3$  nm, respectively. The binary P450cam/Pd complexes were found to have a typical height of about  $(3.9 \div 5.7)$  nm, and the ternary PdR/Pd/P450cam complexes, a typical height of about  $9.1 \pm 0.3$  nm.

## 1 Introduction

Cytochrome P450-containing monooxygenase system plays the key role in the metabolism of drugs, carcinogens, mutagens ect. (1). The cytochrome P450cam (P450cam)-containing monooxygenase system belongs to water-soluble ones and is capable of utilizing this protein for camphor metabolism (2). Elucidation of the operational mechanism of this system is impossible without a detailed knowledge of structure-function relationships in each of its constituent components. It is known that the mechanism underlying the operation of the P450cam system is based on successive transfer of two electrons from putidaredoxin reductase (PdR) to the active centre of cytochrome P450cam (P450cam) through the intermediate redox partner, putidaredoxin (Pd) (3). Once in operation, the system is able to produce both the binary PdR/Pd, Pd/P450cam (4), PdR/P450cam (5) complexes and – as is shown in our optical biosensor studies – the ternary PdR/Pd/P450cam complexes (5). The choice of an adequate model for the interprotein electron transfer realization requires the in-depth structural studies of redox partners and their complexes. By now, of the three proteins comprising the P450cam system, the structures and sizes of only P450cam and Pd have been established: the size of P450cam from x-ray diffraction is 3.3\*5.6\*5.7 nm (6) and the size of Pd, by NMR data, is 3.0\*3.6\*4.0 nm (7). PdR is least studied; thus far, its structure remains unknown. Nor is there any information about the structure of redox partners' complexes; the lack of such data is connected with (a) difficulty in obtaining crystals of protein complexes for x-ray analysis and (b) inherent limitations of the NMR technique. Lately, the atomic force microscopy has been put to use for size measuring and visualization of individual proteins such as chaperonins (8),

microsomal NADPH-cytochrome P450-reductase (Fp) (9) and cytochrome P450<sub>scc</sub> (10). This technique was effectively employed in our earlier study (11) for visualization of cytochrome P450<sub>2B4</sub>/Fp complexes on both hydrophobic (graphite) and hydrophilic (mica) supports in near-native conditions.

The present study was undertaken to demonstrate the AFM potential for investigation of the P450<sub>cam</sub>-containing system comprising three proteins - PdR, Pd, P450<sub>cam</sub> - and for visualization of both the individual proteins and their complexes. Obtained on mica were the images of mostly monomeric PdR, Pd and P450<sub>cam</sub>. Their binary (PdR/Pd, Pd/P450<sub>cam</sub> and PdR/P450<sub>cam</sub>) complexes were also visualized. The imaged complexes' heights were roughly equal to the sum of heights of two (for PdR/Pd and PdR/P450<sub>cam</sub>) and 2 - 3 (for Pd/P450<sub>cam</sub>) redox partners comprising these complexes. Moreover, revealed and visualized were the ternary PdR/Pd/P450<sub>cam</sub> complexes whose heights corresponded to the sum of heights of their constituent (3 - 4) molecules.

## **2 Materials and methods**

### **2.1 Chemicals**

Tris was purchased from Sigma (St.Louis, MO, USA); all other chemicals were from Reakhim (Moscow, Russia). Ultrafiltration of Tris-HCl buffer was carried out in Microcon (Millipore, MA, USA) microconcentrators (membrane molecular weight cut-off = 3 kDa). Ultrapure water was obtained using the Milli-Q system (Millipore, MA, USA).

### **2.2 Preparation of proteins**

Cytochrome P-450cam, putidaredoxin and putidaredoxin reductase were expressed in *E.coli* strain TB, isolated and purified to homogeneity as described elsewhere (12).

### **2.3 Analytical Measurements**

The concentration of P450cam was determined using the extinction coefficient of  $102 \text{ mM}^{-1}\text{cm}^{-1}$  at  $\lambda = 391 \text{ nm}$  (13). The concentrations of purified Pd and PdR were determined with the extinction coefficients of  $10.4 \text{ mM}^{-1}\text{cm}^{-1}$  at  $\lambda = 455 \text{ nm}$  and  $10 \text{ mM}^{-1}\text{cm}^{-1}$  at  $\lambda = 454 \text{ nm}$ , respectively (3).

### **2.4 AFM experiments and samples' preparation**

The experiments were carried out using the direct surface adsorption method (14). As support was used the negatively charged mica surface (SPI, USA). For protein molecule visualization, 5  $\mu\text{l}$  of 0.66  $\mu\text{M}$  solution of appropriate protein in 50 mM Tris

buffer, containing 200 mM KCl, pH 7.4, were deposited onto the mica surface and left for 2 min. Then each sample was rinsed with ultrapure distilled water and dried in airflow. The binary and ternary complexes were obtained by mixing 20  $\mu$ l of 5  $\mu$ M solutions of appropriate individual proteins in the (50 mM Tris + 200 mM KCl) buffer, pH 7.4. Then the mixture was incubated for 10 min, diluted 7.5 times in the same buffer and 5- $\mu$ l portion of the mixture was immediately placed onto mica. The data reported by Guckenberger et al. (15) show that, with relative air humidity exceeding 45%, the mica surface is covered with a water layer. Since in the present study all the measurements were carried out at room temperature and at air humidity 60-70%, the protein molecules under study remained hydrated throughout. The choice of protein concentration was dictated by inherent limitations of the AFM technique – at higher concentrations the molecules under observation formed unbroken layers on the mica support, which excluded the identification of individual objects.

All AFM experiments were carried out in a tapping mode on a multimode Solver P47H atomic force microscope (NT-MDT, Moscow, Russia). The resonant frequency of the cantilevers was 150-250 kHz. The density of protein distribution with height,  $\rho(h)$ , was calculated as  $\rho(h)=(N_h/N)*100\%$ , where  $N_h$  is the number of imaged proteins with the height  $h$ , and  $N$  is the total number of imaged proteins. The calculation was carried out using a step of 0.1 nm and was smoothed off at three points by use of the moving average.

### 3 Results

The AFM proved highly effective in structural studies of biological nanoobjects. This makes the proposed technique an attractive approach for use in proteomic researches. This technique offers an ability to measure, with a high degree of accuracy, the heights of solid objects. At the same time, the AFM-measured lateral sizes of objects appear to be enlarged due to a tip-related effect (16). In this situation, the height of an imaged object was taken as a basic measure of its size and hence as a valid criterion for distinguishing between the monomeric and oligomeric protein forms.

In control experiments, an appropriate buffer mixture without proteins was deposited onto mica and imaged. Randomly distributed contaminations in control measurements were less than 1 nm high.

#### 3.1 AFM visualization of the P450cam, Pd and PdR molecules.

Fig. 1 (A, B, C) presents the AFM images on mica of the isolated P450cam, Pd and PdR molecules, respectively. Distinctly visible in these images are the ellipsoidal objects apparently corresponding to individual. For each molecule type, the distribution density of the number of objects with height - here termed  $\rho(h)$  distribution - was calculated. Such  $\rho(h)$  distributions for P450cam, Pd and PdR are presented in Fig. 2 (A, B, C), respectively. It can be seen that  $82 \pm 4\%$  of imaged **P450cam** molecules have heights between 2.0 and 3.0 nm (Fig. 2A). The  $\rho(h)$  distribution maximum of the imaged objects corresponds to  $h_1 = 2.6 \pm 0.3$  nm. These

objects may be defined as P450cam monomers, since their typical size ( $2.6 \pm 0.3$ ) nm is close to that of P450cam from x-ray diffraction ( $3.3 \times 5.6 \times 5.7$  nm (6)). The fact that the actual size of P450cam is somewhat less than the one from x-ray diffraction is probably explained by the molecule's "contraction" due to probe force.

The majority ( $85 \pm 10\%$ ) of **Pd** images had heights of 1.7 to 2.8 nm (Fig. 2B), with the  $\rho(h)$  maximum at  $h_2 = 2.0 \pm 0.3$  nm; however, there was a minor part ( $9 \pm 5\%$ ) of Pd images with heights 2.8 to 3.7 nm and with the  $\rho(h)$  maximum at  $h = 3.4 \pm 0.3$  nm. It was concluded therefore that Pds mostly occur in the mixture as monomers.

The bulk ( $73 \pm 18\%$ ) of **PdR images** had heights ranging from 2.0 to 5.0 nm (Fig. 2C), with the  $\rho(h)$  maximum at  $h = 2.8 \pm 0.3$  nm. Bearing in mind that the sizes of PdR and P450cam are very similar, it was inferred that the major proportion of PdR images on mica corresponds to monomeric PdRs.

### **3.2 AFM visualization of the binary PdR/Pd, Pd/P450cam and PdR/P450cam complexes**

Binary complexes for visualization experiments were obtained as described under "Materials and Methods". Fig. 3 (A, B, C) presents the imaged objects in the (Pd+P450cam, PdR+Pd) and (PdR+P450cam) mixtures, respectively. Based on the height measurement data, the  $\rho(h)$  distributions of these two groups were calculated.

The  $\rho(h)$  distribution value for the two-component (**Pd+P450cam**) mixture, as compared to the individual P450cam and Pd, is presented in Fig. 4. One can see significant changes in the  $\rho(h)$  distribution curve for the protein mixture as compared to the individual molecules: the proportion of large-sized images with heights 3.9 to 5.7 nm abruptly increased. In the case of the individual proteins, Pd and P450cam, the proportion of objects with height 4 nm and upward did not exceed 6%; however, in the (Pd+P450cam) mixture this proportion was as high as  $51 \pm 16\%$ . As was shown above, the monomeric proteins Pd and P450cam are associated with  $(2.0 \pm 0.3)$ -nm and  $(2.6 \pm 0.3)$ -nm objects, respectively. Therefore, the objects with heights (3.9-5.7) nm and upward may well be considered as complexes between Pd and P450 cam.

A similar situation was observed with the  $\rho(h)$  distribution for the (**PdR+Pd**) mixture (Fig. 5). Here, Fig. 5 (A and B) presents the respective  $\rho(h)$  distributions for the individual PdR and Pd and (C), the  $\rho(h)$  distribution for the (PdR+Pd) mixture. It can be seen that a new maximum of  $\rho(h)$  distribution for PdR+Pd is found at  $4.9 \pm 0.3$  nm; however, no  $\rho(h)$  distribution maximums in this range are to be found with individual proteins. The data obtained were interpreted as hinting at formation of PdR/Pd complexes with height  $4.9 \pm 0.3$  nm.

In our earlier biosensor experiments, the formation of P450cam complexes with PdR was registered (5). Fig. 6 presents the  $\rho(h)$  distribution of the relative number of objects in the (**PdR+P450cam**) mixture. One can see that, along with the contribution to the  $\rho(h)$  value from the monomeric proteins (P450cam and PdR), a substantial contribution to this value comes from objects with a characteristic

height  $5.1 \pm 0.3$  nm. These objects may be apparently identified as PdR/P450cam complexes. Thus, formation of the binary PdR/P450cam complexes in the P450cam system – as was earlier registered by the optical biosensor technique (8) - is now confirmed by direct AFM imaging of these complexes.

### 3.3 AFM visualization of the ternary Pd / PdR / P450cam complexes.

To elucidate whether the ternary complexes are indeed formed in the P450cam system, the AFM images of objects of the (PdR+Pd+P450cam) mixture were obtained (Fig. 7) and the mixture's  $\rho(h)$  distribution was compared with the theoretically calculated sum of the three distributions of objects over their (earlier

measured) heights ( $\sum_{i=1}^3 \rho_i(h)$ ) – for the binary (Pd+PdR), (Pd+P450cam) and

(PdR+P450cam) mixtures (Fig 8). It was found that in the  $\rho(h)$  distribution for the (PdR+Pd+P450cam) mixture the proportion of large-sized objects (with height 6.5 nm and upward) was much greater as compared to  $\sum \rho_i(h)$ :  $26 \pm 3\%$  against  $7 \pm 4\%$ . In other words, the share of ternary PdR/Pd/P450cam complexes among the objects with height 6.5 nm and upward was rather high. Of particular interest is a highly increased (by 7-fold) proportion of  $(9.1 \pm 0.3)$ -nm images compared to the  $\sum \rho_i(h)$ . These images were not observed earlier – either with isolated proteins or with their binary mixtures. Apparently, these 9.1-nm images correspond to ternary complexes, i.e. to aggregates containing molecules of PdR, Pd and P450cam.

## 4 Discussion

It would be of interest to calculate the number of subunit molecules in the AFM-imaged protein complexes (or aggregates) within the P450-containing system. Correct choice of an adequate model for their estimation in a given aggregate or complex is determined by a set of data now available. For the time being we possess no information about the binary or ternary complex sizes in the P450cam-containing system. At first sight, the choice of the spherical model seems preferable.

Based on the spherical model with a molecular mass  $M \sim h^3$ , the degree of aggregation is estimated

$$K = M_1/M_2 = h_1^3/h_2^3, \quad [1]$$

where  $M_1$  and  $M_2$  are the molecular masses of aggregate and monomer, respectively (11).

Using this approach, the number of monomeric molecules in a ternary PdR/Pd/P450cam complex may be calculated. Given that the  $p(h)$  distribution maximum for PdR/Pd/P450cam is to be found at the height = 9.1 nm, the approximate number of monomeric molecules in the complex - in accordance with [1] - constitutes  $(9.1/2.8)^3=34$ , that is each of the largest Pd, PdR and P450cam molecules has a typical height below 2.8 nm.

However, the number of subunits  $n=34$  in a ternary complex (as calculated from the spherical model) seems overestimated: indeed, even in the case of (more

hydrophobic) membrane-bound proteins, cytochrome P450B4, the number of molecules in the aggregate does not exceed 30 (11, 17). It appears therefore that subunit composition in a ternary complex is not adequately described by this model. Apparently, the number of monomeric molecules ( $n$ ) would be determined more correctly by use of the height-summation model. According to this model, the measured height  $h$  of an aggregate (complex) may be represented as the sum of constituent molecules' heights

$$\sum_{i=1}^n h_i = h_1 + h_2 + \dots + h_i \quad (i=1, 2, \dots, n) \quad [2]$$

where  $h_i$  are the heights of images of monomeric proteins. The  $n$  is determined from comparison of  $\sum h$  with an (experimentally measured) height of an aggregate ( $h_a$ ) on condition that

$$\sum h = h_a \quad [3]$$

The heights of the imaged proteins in the P450cam-containing system as well as the heights of their complexes are presented in Table I. As shown above, the most typical height of the ternary PdR/Pd/P450cam complexes is  $9.1 \pm 0.3$  nm. Summing up heights 2.8, 2.0 and 2.6 nm as measured for PdR, Pd and P450cam, respectively, we obtain their  $\sum_{i=3} h = 7.4 \pm 0.9$  nm. The sum of height's maximums for the various combinations of the four molecules  $\sum_{i=4} h$  is equal to  $(9.4 \div 10.2)$  nm, i.e. the heights of complexes comprising 4 molecules, taking into account inaccuracy of measurements, are found in the range 8.2-11.4 nm. From this it follows that the

number of monomeric subunits in a ternary complex does not exceed 3-4 molecules (see Table I).

In the same way, based on the height-summation model, the composition of the imaged binary complexes can be estimated. Comparison of  $h_a$  with the measured heights of the binary (PdR/Pd and PdR/P450cam) complexes allows the conclusion to be drawn that the latter are composed of two different molecule types. In the case of Pd/P450cam complexes, the typical size of their images, (3.9÷5.7) nm, may be obtained from the combination of heights of either two or three monomeric redox partners, Pd and P450cam.

Thus the AFM technique enables to visualize both the individual proteins of water-soluble P450cam system and the redox partners' complexes formed within this system. This approach opens up fresh opportunities for analyzing the molecular organization of cytochrome P450-containing systems containing two (and more than two) redox partners.

## **5 Concluding remarks**

The approach of AFM technique for proteomic investigation of complex multicomponent protein systems was demonstrated. The individual molecules of P450cam, Pd and PdR from the cytochrome P450-containing monooxygenase system were visualized. Also visualized were the functional binary complexes between these molecules. Moreover, the visualization of the ternary PdR/Pd/P450cam complexes in the mixture of these proteins was reported. Among the imaged PdRs, the aggregates of these molecules were revealed. Thus the AFM provides a useful tool for visualization of P450cam, Pd and PdR in isolated and complexed states and hence for a more detailed study of the molecular organization of the P450cam system.

## **6 Acknowledgements**

This work was supported by the Russian Foundation for Basic Research (RFBR) Grants # 99-04-48081, # 00-15-97926, #01-04-48245 and by the Moscow Committee for Science and Technologies (MCST) Grant # 1.2.4. (2001).

## 7 References

1. Archakov, A.I. and Bachmanova, G.P. (1990) Cytochrome P-450 and active oxygen, Taylor & Francis, London, New York, Philadelphia.
2. Bradshaw, W.H., Conrad, H.E., Corey, E.J., Gunsalus, I.C., Lednicer D. (1959) *J. Am. Chem. Soc.* **81**, 5507.
3. Gunsalus, I.C., and Wagner, G.C. (1978) *Methods Enzymol.* **52**, 166-188.
4. Aoki, M., Ishimori, K., and Morishima (1998) *Biochim. Biophys. Acta* **1386 (I)**, 157-167
5. Ivanov, Yu.D., Kanaeva, I.P., Karuzina, I.I., Archakov, A.I., Hui Bon Hoa, H., and Sligar S.G. (2001) *Archives Biochem. Biophys.*, **391**, 2, 255-264.
6. Poulos, T.L., Finzel, B.C., Howard, A.J. (1987) *J. Mol. Biol.* **195**, 687-700.
7. Pochapsky, T.C., Xiao Mei Ye, Ratnaswamy, G., Lyons, T.A. (1994) *Biochemistry* **33**, 6424-6432.
8. Mou, J., Sheng, S.(J.), Ho, R., and Shao, Z. (1996) *Biophysical J.* **71**, 2213-2221.
9. Bayburt, T.H., Carlson, J.W., and Sligar, S.G. (1998) *Journal of Structural Biology* **123**, 37-44.
10. Kiselyova, O.I., Guryev, O.L., Krivosheev, A.V., Usanov, S.A., and Yaminsky, I.V. (1999) *Langmuir* **15**, 1353-1359.
11. Kiselyova, O.I., Yaminsky, I.V., Ivanov, Yu.D., Kanaeva, I.P., Kuznetsov, V.Yu., and Archakov, A.I. (1999) *Archives Biochem. Biophys.* **371**, 1, 1-7.

12. Jung, C., Hui Bon Hoa, G., Schroeder, K.-L., Simon, M., and Doucet, J.P. (1992) *Biochemistry* **31**, 12855- 12862
13. Gunsalus, I.C., and Sligar, S.G. (1978) *Adv. Enzymol. Rel. Areas Mol. Biol.* **47**, 1-44
14. Yang, J., Mou. J., and Shao, Z. (1994) *Biochim. Biophys. Acta* **1199**, 105-114.
15. Guckenberger, R., Heim, M., Cevc, G., Knapp, H.F., Wiegrabe, W., and Hillerbrand, A. (1994) *Science* **266**, 1538-1540.
16. Bustamante, C., Vesenska, J., Tang, C.L., Lees, W., Guthold, M., and Keller, R. (1992) *Biochemistry* **31**, 22-26.
17. Tsuprun, V.L., Myasoedova K.N., Berndt P., Sogra O.N., Orlova E.V., Chernyak V.Ya., Archakov A.I., Skulachev V.P., (1985) *Dokl Akad Nauk* , **285**, 1496-1499.

Table I.

Measured protein complexes heights in P450cam system.

x m	Protein/ Comple	Measured height, nm	Calculated sum of the heights of aggregate-composing monomer proteins ( $\sum h$ ), nm	Number of aggregate-composing protein monomers.
	P450ca	$2.6 \pm 0.3$	$2.6 \pm 0.3$	1
	Pd	$2.0 \pm 0.3$	$2.0 \pm 0.3$	1
	PdR	$2.8 \pm 0.3$	$2.8 \pm 0.3$	1
0cam	Pd/P45	(3.9 - 5.7)	$4.6 \pm 0.6$	2
			$5.7 - 8.1$	3
	PdR/Pd	$4.9 \pm 0.3$	$4.8 \pm 0.6$	2
0cam	PdR/45	$5.1 \pm 0.3$	$5.4 \pm 0.6$	2
450cam	PdR/Pd/	$9.1 \pm 0.3$	$6.5 - 11.4$	3 - 4

## FIGURES

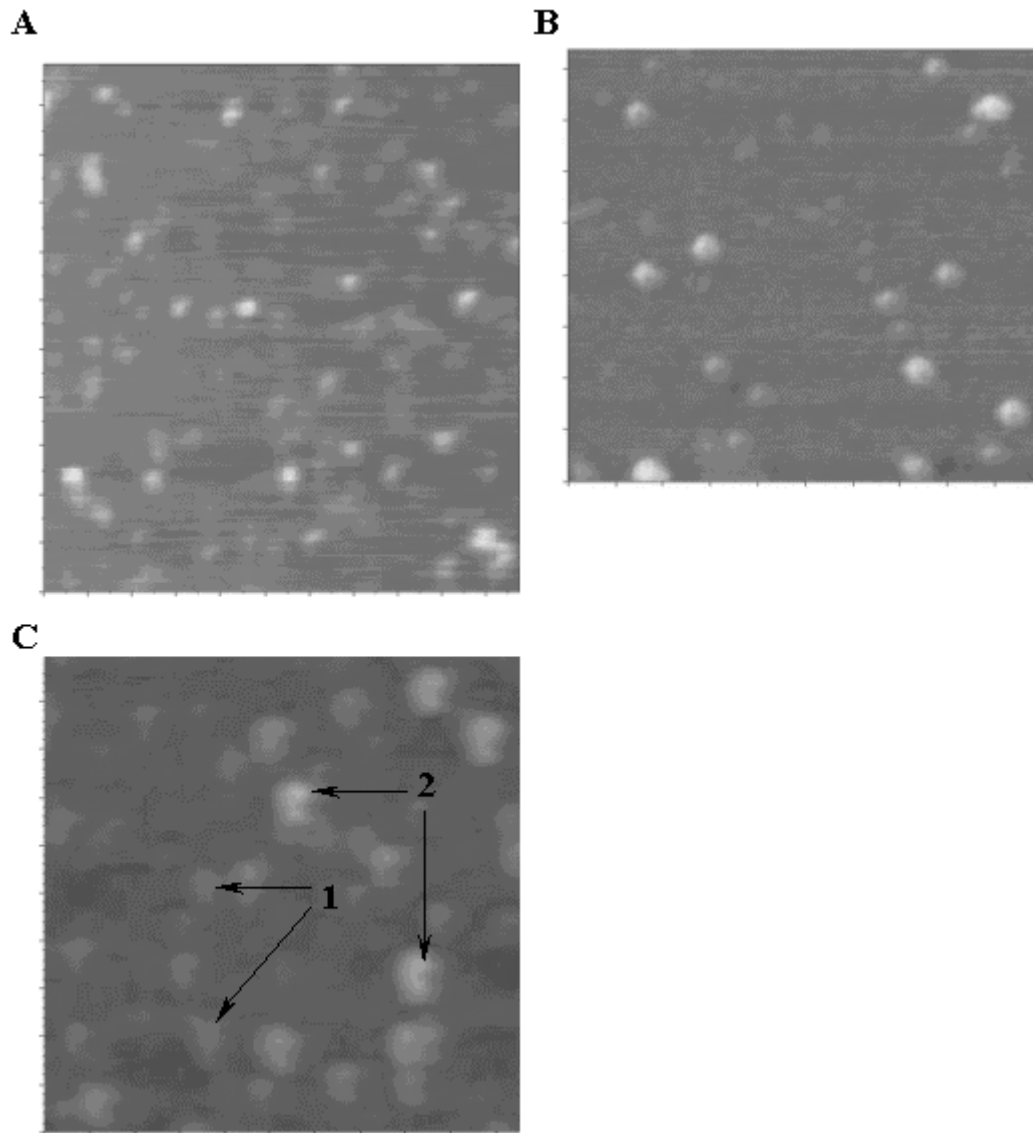


Figure 1: AFM images of P450cam (A), Pd (B) and PdR (C) molecules adsorbed on mica. Tapping mode. Experimental conditions were: 0.66  $\mu\text{M}$  each protein in (50mM Tris + 200 mM KCl) buffer, pH=7.4,  $t=25^\circ\text{C}$ . The image areas were  $0.5 \times 0.5 \mu\text{m}$ . Arrows 1 and 2 indicate, respectively, the images of PdR monomers and aggregates (C).

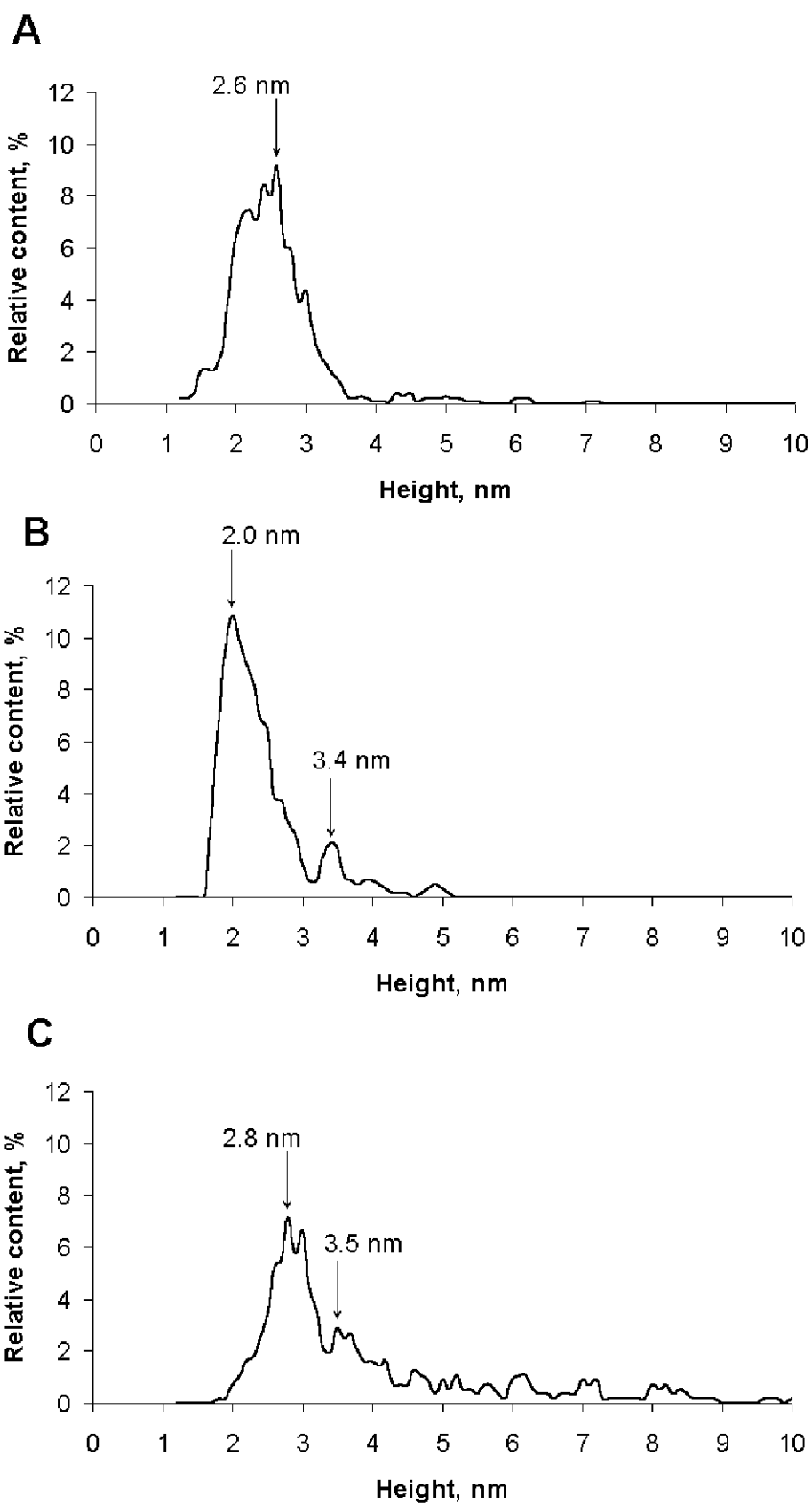


Figure 2: Density of distribution with height,  $p(h)$ , for P450cam (A), Pd (B) and PdR (C), calculated from Figs. 1A, 1B and 1C, respectively.

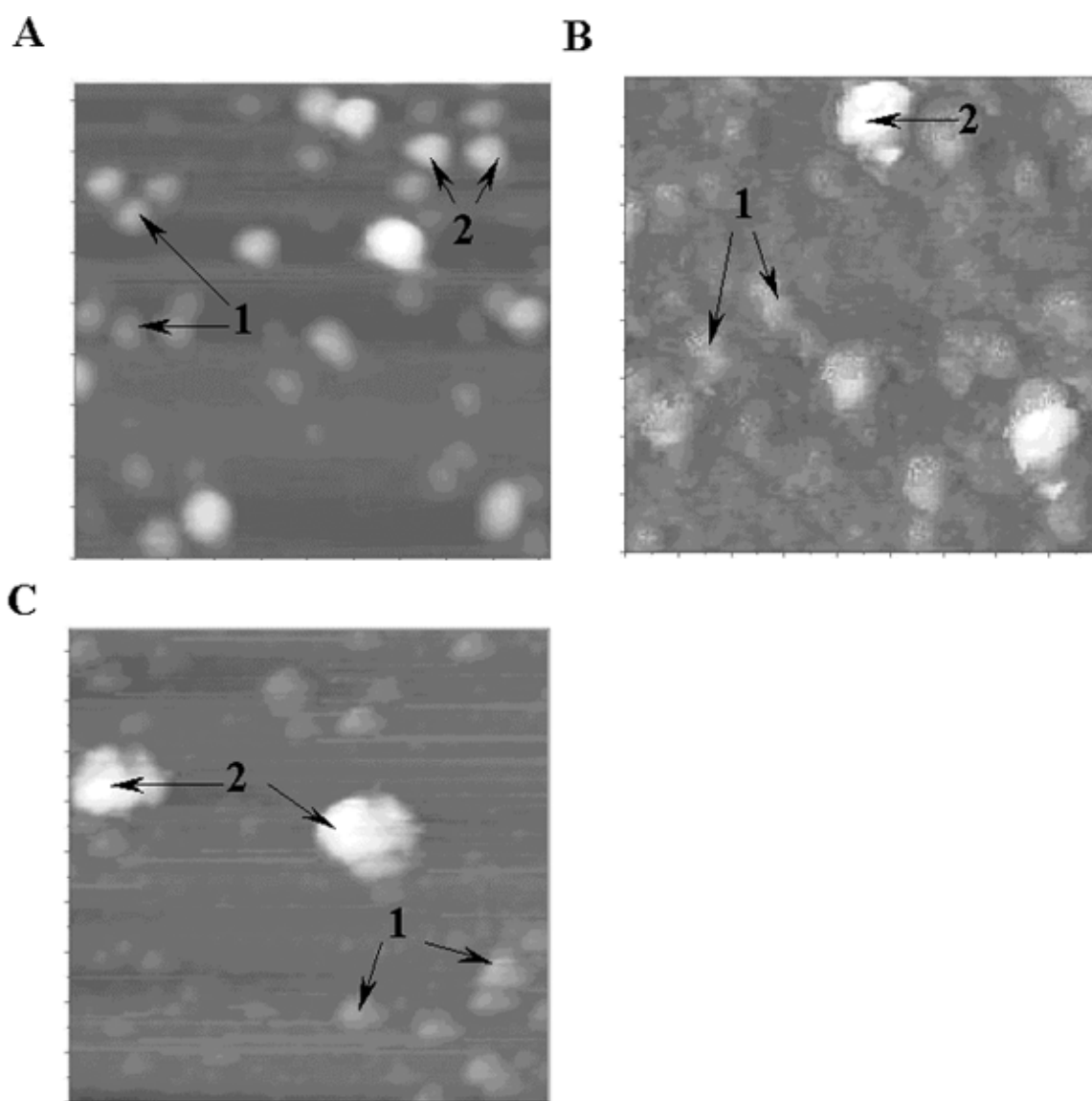


Figure 3: AFM images of the Pd/P450cam (A), PdR/Pd (B) and PdR/P450cam (C) complexes adsorbed on mica. Tapping mode. Experimental conditions were: 0.33  $\mu$ M each protein in (50mM Tris + 200 mM KCl) buffer, pH=7.4,  $t=25^{\circ}\text{C}$ . The image areas were  $0.5 \times 0.5 \mu\text{m}$ . Arrows (1) indicate the images of monomers. Arrows (2) indicate the images of the Pd/P450cam (A), PdR/Pd (B) and PdR/P450cam (C) complexes, respectively.

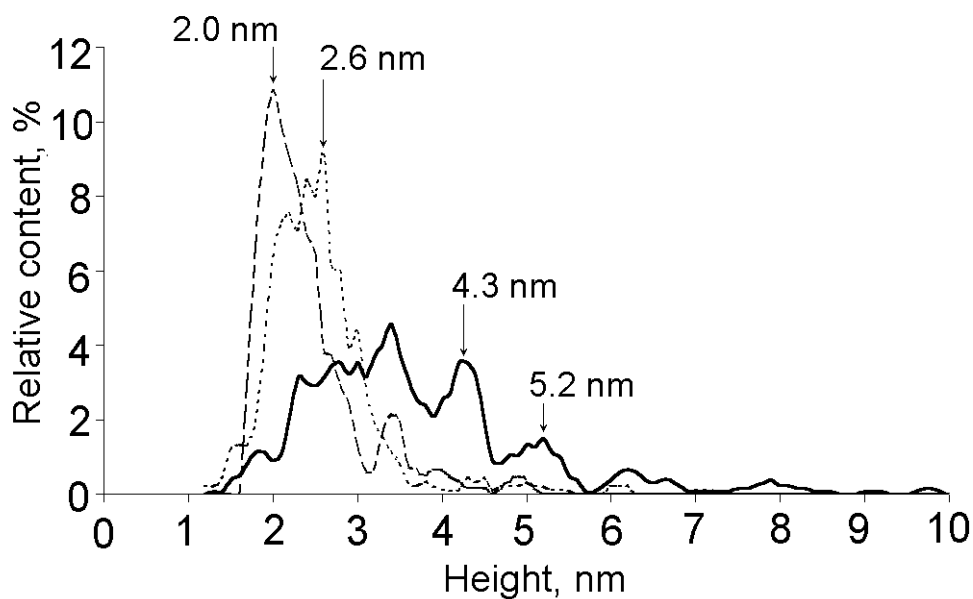


Figure 4: Density of distribution of imaged objects,  $\rho(h)$ , with height for P450cam (dotted line), Pd (dashed line) and for the (Pd + P450cam) mixture (solid line); the latter  $\rho(h)$  is calculated from Fig. 3.

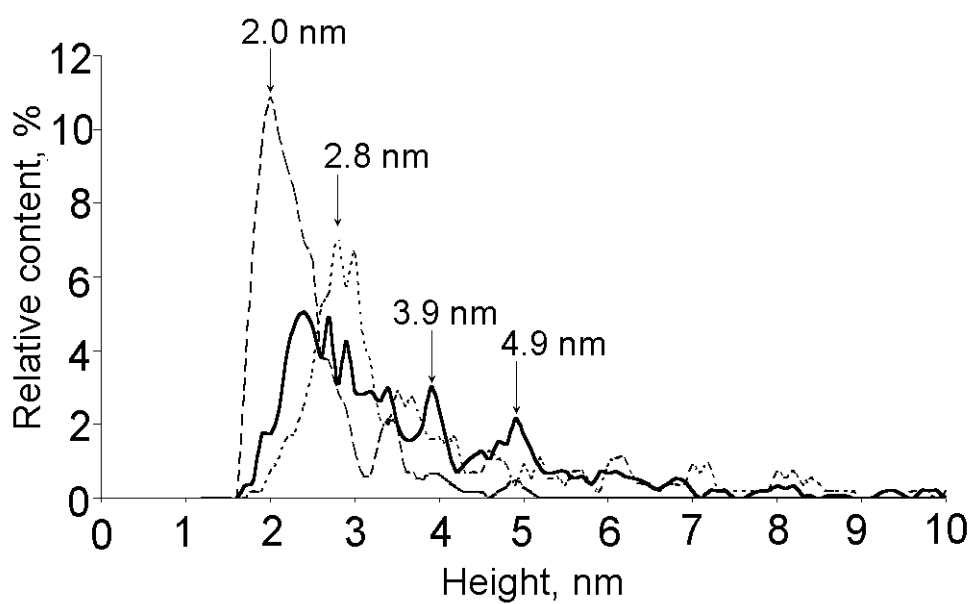


Figure 5: Density of distribution of imaged objects,  $\rho(h)$ , with height for PdR (dotted line), Pd (dashed line) and the (Pd + PdR) mixture (solid line); the latter  $\rho(h)$  is calculated from Fig. 3.

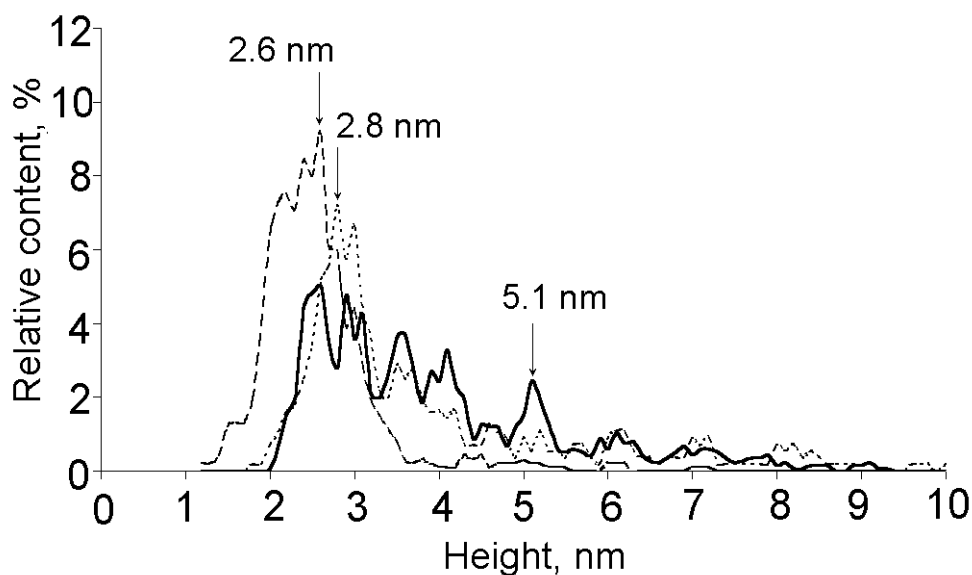


Figure 6: Density of distribution of imaged objects,  $\rho(h)$ , with height for PdR (dotted line), P450cam (dashed line) and the (PdR + P450cam) mixture (solid line); the latter  $\rho(h)$  is calculated from Fig. 3.

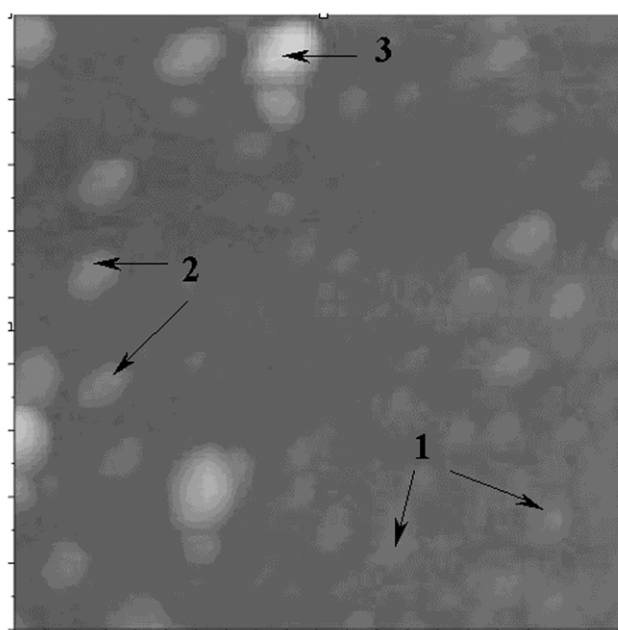


Figure 7: AFM images of P450cam/PdR/Pd complexes adsorbed on mica. Tapping mode. Experimental conditions were:  $0.22 \mu\text{M}$  each protein in (50mM Tris + 200 mM KCl) buffer, pH=7.4;  $t=25^\circ\text{C}$ . The image area was  $0.5 \times 0.5 \mu\text{m}$ . Arrows (1) indicate the images of monomers. Arrows 2 and 3 indicate, respectively, the images of binary and ternary complexes.

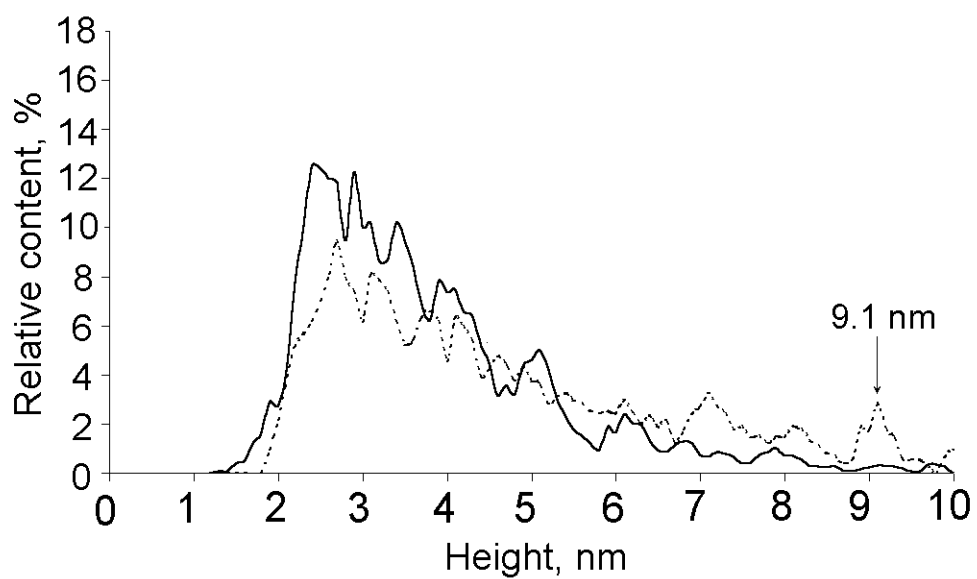


Figure 8: Density of distribution with height,  $\rho(h)$ , for the imaged objects of the (P450cam + PdR + Pd) mixture (dashed lines) - see (Fig. 5), and the triple sum of  $\rho(h)$  distributions for the three binary mixtures (solid lines).

